Chemical Geology 411 (2015) 228–239

Contents lists available at ScienceDirect

Chemical Geology

journal homepage: www.elsevier.com/locate/chemgeo

Impact of atmospheric pCO_2, seawater temperature, and calcification rate on the $\delta^{18}O$ and $\delta^{13}C$ composition of echinoid calcite (*Echinometra viridis*)

T. Courtney [a,b], J.B. Ries [b,*]

[a] Department of Marine Sciences, University of North Carolina at Chapel Hill, Chapel Hill, NC 27599, USA
[b] Marine Science Center, Department of Marine and Environmental Sciences, Northeastern University, 430 Nahant Road, Nahant, MA 01908, USA

ARTICLE INFO

Article history:
Received 8 January 2015
Received in revised form 11 May 2015
Accepted 30 June 2015
Available online 3 July 2015

Editor: Michael E. Böttcher

Keywords:
Stable isotope fractionation
Oxygen
Carbon
Urchin
Echinoid
Ocean acidification
CO_2
Paleothermometer
Calcification

ABSTRACT

The tropical echinoid *Echinometra viridis* was reared in controlled laboratory experiments at temperatures of approximately 20 °C and 30 °C to mimic winter and summer temperatures and at carbon dioxide (CO_2) partial pressures of approximately 487 ppm-v and 805 ppm-v to simulate current and predicted-end-of-century levels. Spine material produced during the experimental period and dissolved inorganic carbon (DIC) of the corresponding culture solutions were then analyzed for stable oxygen ($\delta^{18}O_e$, $\delta^{18}O_{DIC}$) and carbon ($\delta^{13}C_e$, $\delta^{13}C_{DIC}$) isotopic composition. Fractionation of oxygen stable isotopes between the echinoid spines and DIC of their corresponding culture solutions ($\Delta^{18}O = \delta^{18}O_e - \delta^{18}O_{DIC}$) was significantly inversely correlated with seawater temperature but not significantly correlated with atmospheric pCO_2. Fractionation of carbon stable isotopes between the echinoid spines and DIC of their corresponding culture solutions ($\Delta^{13}C = \delta^{13}C_e - \delta^{13}C_{DIC}$) was significantly positively correlated with pCO_2 and significantly inversely correlated with temperature, with pCO_2 functioning as the primary factor and temperature moderating the pCO_2–$\Delta^{13}C$ relationship. Echinoid calcification rate was significantly inversely correlated with both $\Delta^{18}O$ and $\Delta^{13}C$ across treatments, with effects of pCO_2 and temperature controlled for through ANOVA. Therefore, calcification rate and potentially the rate of co-occurring dissolution appear to be important drivers of the kinetic isotope effects observed in the echinoid spines. Study results suggest that echinoid $\Delta^{18}O$ monitors seawater temperature, but not atmospheric pCO_2, and that echinoid $\Delta^{13}C$ monitors atmospheric pCO_2, with temperature moderating this relationship. These findings, coupled with echinoids' long and generally high-quality fossil record, support prior assertions that fossil echinoid $\Delta^{18}O$ is a viable archive of paleo-seawater temperature throughout Phanerozoic time, and that $\Delta^{13}C$ merits further investigation as a potential proxy of paleo-atmospheric pCO_2. However, the apparent impact of calcification rate on echinoid $\Delta^{18}O$ and $\Delta^{13}C$ suggests that paleoceanographic reconstructions derived from these proxies in fossil echinoids could be improved by incorporating the effects of growth rate.

1. Introduction

The stable isotopic compositions of calcium carbonate minerals ($\delta^{13}C$, $\delta^{18}O$) are known to record changes in ocean temperature and atmospheric pCO_2 that have occurred throughout Earth history (e.g., Berner, 1990; Emiliani, 1955; Petit et al., 1999; Shackleton et al., 1983; Veizer et al., 2000; Weaver et al., 1997). Echinoids are globally distributed benthic calcifiers with a relatively long fossil record, dating back to the Lower Cambrian (e.g., Lebrato et al., 2010; Paul and Smith, 1984). They also tend to be well preserved in the fossil record owing to the hydrophobic organic matter that encapsulates their spines and plates (Dickson, 2002, 2004; O'Malley et al., 2013) and inhibits diagenetic resetting of their stable isotopic signatures, rendering echinoids a potentially valuable geochemical archive of ancient seawater conditions.

Numerous studies have investigated the impacts of seawater temperature on oxygen and carbon isotope fractionation within echinoderm Mg-calcite (e.g., Baumiller, 2001; Gorzelak et al., 2012; Richter and Bruckschen, 1998; Weber, 1968). Analysis of 116 modern ophiuroid (brittle star) skeletons showed a positive correlation between $\delta^{13}C$ and temperature, a negative correlation between $\delta^{18}O$ and temperature, and a weakly positive correlation between $\delta^{13}C$ and $\delta^{18}O$ (Weber, 1968). A negative correlation between $\delta^{18}O$ and temperature was also observed for modern crinoids with no significant correlation between $\delta^{13}C$ and temperature (Weber, 1968). In addition to observing a negative correlation between $\delta^{18}O$ and temperature, Gorzelak et al. (2012) also noted a weak positive correlation between $\delta^{13}C$ and $\delta^{18}O$ within the extant crinoid *Metacrinus rotundus*, which they asserted may have been confounded by metabolic factors such as respiration and/or diet. Richter and Bruckschen (1998) found the $\delta^{18}O$ of tests of the echinoid *Echinocyamus pusillus* to be positively correlated with salinity, negatively correlated with meteoric water input, and negatively correlated with temperature. Collectively, these results suggest that echinoderm $\delta^{18}O$

* Corresponding author.
E-mail address: j.ries@neu.edu (J.B. Ries).

http://dx.doi.org/10.1016/j.chemgeo.2015.06.030
0009-2541/

may provide a useful proxy of paleoseawater temperature, while the potential impacts of seawater temperature on echinoderm $\delta^{13}C$ may be complicated by other environmental and/or metabolic factors that affect carbon isotope fractionation.

Equilibrium fractionation of oxygen and carbon isotopes occurs among species of dissolved inorganic carbon (DIC) as a function of seawater temperature once isotopic equilibrium is reached (e.g., McCrea, 1950). Abiotic precipitation experiments have confirmed that $\delta^{18}O$ (e.g., Beck et al., 2005; Wang et al., 2013; McCrea, 1950) and $\delta^{13}C$ (McCrea, 1950; Zhang et al., 1995) of seawater DIC species vary inversely with temperature in a manner consistent with equilibrium isotope fractionation. However, abiogenic calcite precipitation experiments performed by Romanek et al. (1992) revealed calcite to be approximately 1‰ enriched in ^{13}C relative to HCO_3^- with no significant correlations between $\delta^{13}C$ and temperature, indicating that kinetic factors can lead to disequilibrium fractionation of carbon and oxygen isotopes even in abiotically precipitated carbonates.

Carbon and oxygen isotopic disequilibrium has also been observed in numerous studies of biogenic carbonates, apparently due to the biological processes involved in calcification (Adkins et al., 2003; Bemis et al., 2000; Gorzelak et al., 2012; McConnaughey, 1989a; Weber, 1968; Weber and Raup, 1966; Zeebe, 1999). Adkins et al. (2003) proposed a novel vital effect for the deepwater corals *Desmophyllum cristagalli* and *Lophelia* sp., in which apparent isotopic disequilibrium of $\delta^{13}C$ is established by mixing of carbon reservoirs driven by a pH gradient across the cell membrane at the site of calcification, with $\delta^{18}O$ disequilibrium driven by pH induced DIC speciation. Bemis et al. (2000) observed the calcite of the foraminifera *Orbulina universa* to have $\delta^{13}C$ that is approximately 1‰ more positive than seawater DIC when grown in low light conditions and attributed this disequilibrium to kinetic isotope effects arising from selective uptake of lighter isotopes by organic matrices surrounding the site of calcification. Rates of calcification have also been shown to impart kinetic isotope effects, resulting in shell $\delta^{13}C$ that is up to 10–15‰ lighter than seawater DIC and shell $\delta^{18}O$ that is up to 4‰ lighter than seawater DIC (McConnaughey, 1989a). Negative correlations have also been observed between rates of respiration and $\delta^{13}C$ of seawater DIC (McConnaughey, 1989a).

Because echinoderms lack structurally complex respiratory systems, perivisceral coelomic fluids must transport respired CO_2 throughout the organism (Weber, 1968). Stumpp et al. (2012) also demonstrated that larval echinoids have a leaky integument, indicating that their intracellular fluid is exposed to changes in the pH of their extracellular fluid, which is directly impacted by pH changes in ambient seawater—although they also demonstrated that echinoids are able to control pH of their intracellular fluid. Collectively, these studies indicate that ambient seawater (heavier isotope signal) and respired seawater (lighter isotope signal) are mixed within the echinoderm tissue, suggesting that seawater pH, growth rate, and respiration are all important factors to consider when investigating the source of isotopic disequilibrium in biogenic carbonates such as echinoid spines.

Prior studies have also investigated phylogenetic and intraspecimen variability in the stable isotopic disequilibria ($\delta^{13}C$, $\delta^{18}O$) of echinoderm skeletons (Gorzelak et al., 2012; Weber and Raup, 1966; Weber and Raup, 1968). A study of 45 families of fossil echinoderms found that the $\delta^{13}C$ and $\delta^{18}O$ composition of their tests varied among families, as well as among different skeletal elements within individuals (Weber and Raup, 1968). That study concluded that the overall variation in the stable isotopic composition of echinoderms has increased throughout geologic time as the phylum diversified (Weber and Raup, 1968). Gorzelak et al. (2012) also identified approximately 10‰ variations in $\delta^{13}C$ among clades of crinoids and significant variability in the stable isotopic composition of extant crinoids—across species, across individuals within a given species, and across skeletal elements within a given individual. Likewise, Weber and Raup (1966) found that aboral spines of *Echinometra lucunter* are enriched in ^{13}C and ^{18}O relative to spines located closer to the mouth and that tests were generally depleted in ^{13}C and ^{18}O relative to spines. They also found no significant variation in stable isotopic composition across the length of the spine. These studies reveal variability in echinoderm $\delta^{18}O$ and $\delta^{13}C$ across species, individuals, and skeletal elements. This variability must be taken into account when employing these isotopes in paleoceanographic reconstructions.

Although Weber (1973) originally proposed that echinoids are prone to diagenesis and thus poorly suited for paleoceanographic reconstructions, Dickson (2002, 2004) found echinoderm stereom calcite to be unusually well preserved throughout the geologic record owing to its encasement in hydrophobic organic matter. Echinoderms' unique quality of preservation in the fossil record enabled Dickson to reconstruct the Phanerozoic history of seawater Mg/Ca from the Mg/Ca of fossil echinoderms. Although Hasiuk and Lohmann (2008) determined that early diagenetic alteration caused crinoid skeletal $\delta^{13}C$ and $\delta^{18}O$ to initially converge on isotopic compositions of their surrounding cement, they also concluded that this process of early alteration ultimately protected the crinoid skeletons from more severe, subsequent alteration. Well-preserved echinoderm-specific organic molecules found in Mississippian-age (340 Ma) crinoid fossils (O'Malley et al., 2013) further support Dickson's conclusions that echinoderm skeletal material may be geochemically preserved over geologic time scales. O'Malley et al. (2013) attributed the crinoids' high quality preservation to their deposition in fine-grained sediments that inhibited the flow of diagenetic fluids, and also to the absence of metamorphism at the crinoid collection site. These findings collectively suggest that well-preserved fossilized echinoderms are a potentially valuable and relatively underutilized archive of paleoceanographic conditions.

The objective of the present study is to investigate the impact of seawater temperature and atmospheric pCO_2 on the $\delta^{13}C$ and $\delta^{18}O$ composition of Mg-calcite produced by *Echinometra viridis*, a cryptic rock- and reef-dwelling echinoid found throughout the Caribbean Sea (McPherson, 1969). The results of the present study reveal the utility and limitations of echinoid $\delta^{13}C$ and $\delta^{18}O$ as a proxy of paleoseawater temperature and atmospheric pCO_2 and provide insight into the mechanisms of echinoid calcification.

2. Materials and methods

2.1. Echinoid culture experiment

Approximately 44 specimens of the tropical echinoid *E. viridis* were collected near Key Largo in southern Florida and reared for 60 days in a three-way replicated two-way factorial experiment in which low (circa 487 ppm-v) and high (circa 805 ppm-v) pCO_2 treatments were crossed with low (circa 20 °C) and high temperature treatments (circa 30 °C; see Courtney et al., 2013, for detailed methods). In brief, the urchins were reared in 34 L aquaria filled with seawater of salinity 32.06 (SE = 0.02), formulated from deionized water mixed with *Instant Ocean Sea Salt*—identified in a prior study as the commercial sea salt that best replicates the chemical composition of natural seawater (Atkinson and Bingham, 1998). The aquaria were filtered at 757 L/h with activated carbon in a floss-filter cartridge and illuminated for 10 h/day at 884 (SE = 38) Lux. Experimental aquaria were allowed to equilibrate with the bubbled gas mixture for 24-h prior to the beginning of the rearing experiment. The echinoids were fed to satiation every other day with approximately 60 mg of dehydrated marine green algae per tank. Net calcification rates were estimated from changes in the echinoids' buoyant weight between the beginning and end of the experiment. Details regarding application of the buoyant weight method to estimating net calcification rates of echinoids are available in the supplementary information of Ries et al. (2009).

The actual pCO_2 and temperature for the four treatments (±SE) were: (1) 20.3 ± 0.1 °C and 524 ± 33 ppm-v; (2) 20.6 ± 0.1 °C and

827 ± 37 ppm-v; (3) 30.0 ± 0.1 °C and 448 ± 27 ppm-v; and (4) 29.9 ± 0.1 °C and 783 ± 45 ppm-v (Table 1). The low-temperature treatments were circulated and cooled by pumping the aquarium seawater through tubes coiled in a sufficiently low temperature water bath maintained by a 1 HP aquarium chiller. The high-temperature treatments were maintained with 50 W heaters and circulated with powerheads at 400 L/h. The low-pCO_2 gas was supplied to the laboratory through an in-house compressor and was sourced from air outside of the laboratory building. The high-pCO_2 gas was formulated by mixing pure compressed CO_2 gas with the low-pCO_2 gas using digital, solenoid-valve mass flow controllers. The gases were bubbled into the aquaria via 6-inch porous ceramic airstones that were secured to the bottom of each aquarium. Gas pCO_2 (Table 1) was measured with a *Qubit* S151 infrared pCO_2 analyzer calibrated with certified air–CO_2 gas standards and commercial air–CO_2 gas mixtures (calibrated using certified air–CO_2 gas standards; precision = ±2.0%; accuracy = ±1.8%).

Temperature within the experimental aquaria (Table 1) was measured every other day with a NIST-calibrated partial-immersion organic-filled glass thermometer. Seawater pH (Table 1) was measured every other day with a *Thermo Scientific Orion 2 Star* benchtop pH meter and an *Orion 9156BNWP* probe, calibrated with certified NBS 7.00 and 10.01 *Orion* buffers (for slope of the calibration curve) and with seawater standards of known pH provided by the laboratory of Prof. A. Dickson of Scripps Institution of Oceanography (for y-intercept of the

Table 1
Summary of measured and calculated seawater parameters for each experimental treatment.

Measured values					
pCO_2	(ppm-v)	487	800	488	801
	SE	1	1	1	1
	Range	481–493	796–804	482–494	795–805
	n	9	9	9	9
Temp	(°C)	20.3	20.6	30.0	29.9
	SE	0.1	0.1	0.1	0.1
	Range	19.3–21.2	19.9–21.6	29.5–30.6	29.3–30.4
	n	27	27	27	27
Sal	(psu)	32.00	32.07	32.12	32.07
	SE	0.03	0.02	0.06	0.04
	Range	31.60–32.40	31.80–32.40	31.00–32.90	31.60–32.60
	n	27	27	27	27
pH		8.23	8.00	8.34	8.11
	SE	0.01	0.01	0.01	0.01
	Range	8.17–8.29	7.83–8.05	8.26–8.42	8.04–8.20
	n	27	27	27	27
TA	(μM)	3383	3574	3289	3335
	SE	29	27	35	44
	Range	3157–3738	3289–3905	2785–3568	2837–3678
	n	27	27	27	27
DIC	(μM)	2979	3304	2744	2951
	SE	17	18	32	37
	Range	2785–3114	3148–3435	2367–3057	2490–3209
	n	27	27	27	27
$\delta^{18}O_{DIC}$	(‰ V-PDB)	−3.55	−3.30	−2.88	−3.29
	SE	0.08	0.09	0.11	0.12
	Range	−3.91 to −3.25	−3.59 to −2.78	−3.28 to −2.18	−3.77 to −2.74
	n	9	9	9	8
$\delta^{13}C_{DIC}$	(‰ V-PDB)	−6.67	−15.69	−5.90	−13.83
	SE	0.36	0.17	0.29	0.16
	Range	−8.33 to −4.25	−16.17 to −14.60	−6.90 to −4.25	−15.70 to −14.24
	n	9	9	9	7
Calculated values					
$pCO_{2\ (gas\text{-}e)}$	(ppm-v)	524	827	448	783
	SE	33	37	27	45
	Range	272–950	445–1137	240–713	479–1495
	n	27	21	27	27
pH		8.25	8.04	8.29	8.10
	SE	0.02	0.03	0.02	0.02
	Range	7.99–8.49	7.68–8.34	8.10–8.51	7.85–8.30
	n	27	27	27	27
$[CO_3^{2-}]$	(μM)	330	241	437	320
	SE	16	14	16	13
	Range	189–527	106–437	300–645	180–485
	n	27	27	27	27
$[HCO_3^-]$	(μM)	2632	3031	2296	2611
	SE	21	20	37	34
	Range	2444–2842	2849–3247	2016–2650	2199–2867
	n	27	27	27	27
$[CO_2]_{(SW)}$	(μM)	17	32	11	20
	SE	1	2	1	1
	Range	9–30	15–73	6–18	12–38
	n	27	27	27	27
Ω_A		5.2	3.8	7.2	5.3
	SE	0.3	0.2	0.3	0.2
	Range	3.0–8.3	1.7–6.9	5.0–10.7	3.0–8.1
	n	27	27	27	27

calibration curve). A *VINDTA 3C* (*MARIANDA* corporation) was used to make weekly measurements of DIC via coulometry (*UIC 5400*) and total alkalinity (TA) via closed-cell potentiometric titration (Table 1). The program CO_2SYS (Lewis and Wallace, 1998) was used to calculate the other seawater carbonate system parameters (Table 1) using measured seawater temperature, pH, salinity, and alkalinity, Roy et al. (1993) values for the K_1 and K_2 carbonic acid constants, the Mucci (1983) value for the stoichiometric aragonite solubility product, and an atmospheric pressure of 1.015 atm. Measured pCO_2 of the introduced gases was within 7.5%, 3.4%, 8.1%, and 2.2% of equilibrium pCO_2 calculated from the measured carbonate system parameters for the 20.3 °C/524 ppm-v, 20.6 °C/827 ppm-v, 30.0 °C/448 ppm-v, and 29.9 °C/783 ppm-v treatments, respectively (Table 1)—indicating that the experimental seawaters were near equilibrium with the introduced gases. Since the gas–water equilibration time is orders of magnitude longer than the time required to establish isotopic equilibrium between the various DIC pools, the isotopic composition of the DIC pools should be even closer to equilibrium than the gas–seawater systems. Nevertheless, it should be noted that any isotopic disequilibrium between the DIC species within the experimental seawaters, no matter how small, may limit application of the study results to reconstructing temperature and pCO_2 for a natural seawater system with DIC reservoirs that are closer to isotopic equilibrium.

2.2. Spine sampling and preparation

Three to five spines up to approximately 5 mm in length were sampled from anatomically equivalent zones of newly formed spines around the echinoids' mouths to ensure that the sampled material was produced exclusively under the experimental conditions. Spines of a given echinoid specimen were combined and gently ground to a fine powder for approximately 30 s using an agate mortar and pestle, which was cleaned with a 1 M hydrochloric acid solution and then rinsed with 95% ethanol between samples. The ground spines of each echinoid were then subsampled and analyzed for their stable isotopic composition ($\delta^{18}O$, $\delta^{13}C$).

2.3. $\delta^{18}O$ and $\delta^{13}C$ mass spectrometry

Echinoid spines and dissolved inorganic carbon (DIC) of weekly seawater samples were analyzed for their $\delta^{18}O$ and $\delta^{13}C$ composition at the Keck Paleoenvironmental and Environmental Stable Isotope Laboratory within University of Kansas' Department of Geology (Table 2). Approximately 119 (SE = 4) μg of powdered spine material was analyzed per echinoid. Spine material was placed in *Exetainer* vials and flushed with ultra-high purity helium for 5 min. Each echinoid sample was then reacted with 3–4 drops of 100% phosphoric acid for 24 h at 25 °C to liberate all CO_2 from the echinoid spine material. One mL seawater samples (9 weekly subsamples from each of the four treatments, n = 36) were reacted with 5 drops of 98% phosphoric acid at 25 °C in rubber-septum-sealed *Exetainer* vials flushed for 5 min with ultra-high purity helium, and allowed to equilibrate for 20 h prior to analysis. The liberated CO_2-gas was analyzed using a *ThermoFinnigan GasBench II* with an in-line *Finnigan MAT 253* isotope ratio mass spectrometer in continuous flow mode. The software *Isodat* was used to analyze five peaks per sample. $\delta^{18}O$ and $\delta^{13}C$ for each set of samples were calculated from the last four peaks of each analysis. An acid fractionation factor of 1.01025 (cf. Zeebe and Wolf-Gladrow, 2001) was used to correct the $\delta^{18}O$ measurements of CO_2 liberated through reaction with phosphoric acid.

The isotope ratio mass spectrometer system was calibrated with NIST standards NBS-18 (Carbonatite Reference Material #8543) and NBS-19 (Limestone Reference Material #8544), as well as internal standards (Calcite-1 and Merck Calcium Carbonate [B753159]) before and after each sample queue. NIST standards NBS-18 and NBS-19, NIST reference material 88b (dolomitic limestone), and the internal standards were analyzed every ten samples for quality control. This procedure

Table 2
Summary of pCO_2, temperature, calcification rate (%-change in buoyant weight per 60-days), $\delta^{18}O_{DIC}$, δ^{13}_{DIC}; $\delta^{18}O_e$, $\delta^{13}C_e$, $\Delta^{18}O$, and $\Delta^{13}C$ for individual echinoid specimens. $\delta^{18}O_{DIC}$ and $\delta^{13}C_{DIC}$ are the average stable isotopic composition of 9 water samples per treatment, collected weekly throughout the duration of the experiment. $\delta^{13}C_{DIC}$ of the high-pCO_2 treatments were greater than $\delta^{13}C_{DIC}$ of the low-pCO_2 treatments because of the relatively light $\delta^{13}C$ composition of the methane-derived CO_2 source-gas compared with the compressed air obtained from outside of the laboratory that was used in the low-pCO_2 treatments. These differences in $\delta^{13}C_{DIC}$ among treatments were normalized by expressing isotope effects as the difference in $\delta^{13}C$ between the echinoid calcite and DIC of the culture solution (i.e., $\Delta^{13}C = \delta^{13}C_e - \delta^{13}C_{DIC}$).

pCO_2 (ppm-v)	Temperature (°C)	Calcification rate (%)	$\delta^{18}O_{DIC}$ (‰ V-PDB)	$\delta^{13}C_{DIC}$ (‰ V-PDB)	$\delta^{18}O_e$ (‰ V-PDB)	$\delta^{13}C_e$ (‰ V-PDB)	$\Delta^{18}O$ (‰ V-PDB)	$\Delta^{13}C$ (‰ V-PDB)
444	29.7	30.25	−2.88	−5.90	−2.43	−1.64	0.45	4.26
444	29.7	23.96	−2.88	−5.90	−2.83	−0.20	0.05	5.70
449	30.2	−0.19	−2.88	−5.90	−2.82	−1.79	0.06	4.11
449	30.2	24.84	−2.88	−5.90	−1.95	0.14	0.93	6.04
449	30.2	7.19	−2.88	−5.90	−1.05	−0.13	1.83	5.77
452	30.1	13.44	−2.88	−5.90	−1.72	−0.08	1.16	5.82
452	30.1	11.50	−2.88	−5.90	−1.00	−1.47	1.88	4.43
489	19.7	0.98	−3.55	−6.67	−0.95	0.57	2.60	7.24
523	20.2	4.75	−3.55	−6.67	−1.15	0.79	2.40	7.46
523	20.2	−15.92	−3.55	−6.67	−1.02	0.79	2.53	7.46
523	20.2	18.41	−3.55	−6.67	−1.71	−1.44	1.84	5.23
559	20.9	−2.00	−3.55	−6.67	−0.99	−2.42	2.56	4.25
559	20.9	4.76	−3.55	−6.67	−1.49	−2.53	2.06	4.14
559	20.9	−1.71	−3.55	−6.67	−1.00	0.46	2.55	7.13
777	29.6	25.03	−3.29	−13.83	−2.65	−5.01	0.64	8.82
777	29.6	11.47	−3.29	−13.83	−2.63	−5.70	0.66	8.13
777	29.6	9.39	−3.29	−13.83	−1.15	−2.50	2.14	11.33
733	30.0	1.79	−3.29	−13.83	−4.23	−9.09	−0.94	4.74
733	30.0	1.74	−3.29	−13.83	−3.64	−8.05	−0.35	5.78
733	30.0	−20.95	−3.29	−13.83	−0.88	0.62	2.41	14.45
838	29.9	−5.30	−3.29	−13.83	−1.40	−3.25	1.89	10.58
838	29.9	7.88	−3.29	−13.83	−1.02	−1.89	2.27	11.94
788	20.3	9.32	−3.30	−15.69	−1.67	−5.13	1.63	10.56
788	20.3	−38.54	−3.30	−15.69	−0.82	0.42	2.48	16.11
788	20.3	−9.82	−3.30	−15.69	−1.81	−4.31	1.49	11.38
839	20.5	−29.86	−3.30	−15.69	−0.94	−0.28	2.36	15.41
860	20.8	−20.29	−3.30	−15.69	−0.55	0.58	2.75	16.27
860	20.8	1.76	−3.30	−15.69	−0.73	0.54	2.57	16.23

Table 3
Summary of ANOVA statistics for T vs. $\Delta^{18}O$, pCO_2 vs. $\Delta^{18}O$, T vs. $\Delta^{13}C$, pCO_2 vs. $\Delta^{13}C$, $\Delta^{13}C$ vs. T + pCO_2, $\Delta^{18}O$ vs. $\Delta^{13}C$, $\Delta^{18}O$ vs. $\Delta^{13}C$ + calcification rate, $\Delta^{18}O$ vs. $\Delta^{13}C$ + pCO_2 + T, $\Delta^{18}O$ vs. $\Delta^{13}C$ + pCO_2 + T + calcification rate, $\Delta^{18}O$ vs. calcification rate + T + pCO_2, and $\Delta^{13}C$ vs. calcification rate + T + pCO_2 .

ANOVA	Predictor	Value	SE	F-value	*p*-Value
T vs. $\Delta^{18}O$	$\Delta^{18}O$	−2.9	0.7	17.138	0.0003
pCO_2 vs. $\Delta^{18}O$	$\Delta^{18}O$	30	30	0.75	0.393
T vs. $\Delta^{13}C$	$\Delta^{13}C$	−0.4	0.2	2.69	0.113
pCO_2 vs. $\Delta^{13}C$	$\Delta^{13}C$	31	5	43.71	<0.0001
$\Delta^{13}C$ vs. T + pCO_2	Temperature	−0.2	0.1	7.03	0.014
	pCO_2	0.019	0.003	42.91	<0.0001
$\Delta^{18}O$ vs. $\Delta^{13}C$	$\Delta^{18}O$	2.0	0.7	8.97	0.006
$\Delta^{18}O$ vs. $\Delta^{13}C$ + calcification rate	$\Delta^{13}C$	0.08	0.05	1.52	0.006
	Calcification rate	−0.02	0.01	−1.28	0.21
$\Delta^{18}O$ vs. $\Delta^{13}C$ + pCO_2 + T	$\Delta^{13}C$	0.19	0.06	15.17	0.0007
	pCO_2	−0.003	0.001	8.62	0.007
	Temperature	−0.10	0.02	11.34	0.003
$\Delta^{18}O$ vs. $\Delta^{13}C$ + pCO_2 + T + calcification rate	$\Delta^{13}C$	0.18	0.06	14.56	0.0009
	pCO_2	−0.003	0.001	8.27	0.009
	Temperature	−0.10	0.03	10.88	0.003
	Calcification rate	0.00	0.01	0.029	0.87
$\Delta^{18}O$ vs. calcification rate + T + pCO_2	Calcification rate	−0.02	0.01	10.29	0.004
	Temperature	−0.11	0.04	8.95	0.006
	pCO_2	0.000	0.001	0.02	0.89
$\Delta^{13}C$ vs. calcification rate + T + pCO_2	Calcification rate	−0.08	0.03	5.12	0.03
	Temperature	−0.1	0.1	8.19	0.009
	pCO_2	0.016	0.003	49.98	<0.0001

yielded precisions better than 0.06 and 0.12‰ for $\delta^{13}C$ (V-PBD) and $\delta^{18}O$ (V-PBD), respectively.

The lack of certified standards for $\delta^{18}O$ of seawater (or freshwater) DIC required calibration of the DIC $\delta^{18}O$ analyses using the same suite of solid carbonate standards described above. Although calibrating $\delta^{18}O$ analyses of seawater DIC using non-seawater standards is not ideal, Beck et al. (2005) showed that such 'acid stripping' of DIC from seawater can yield $\delta^{18}O$ values for seawater DIC that are consistent with other methods. Quality control for this method was assessed via repeat analyses of an internal seawater standard with seawater $\delta^{18}O$ calibrated against certified NIST standards VSMOW2 and SLAP. The DIC $\delta^{18}O$ of the internal standard was then calculated from the measured seawater $\delta^{18}O$ of the internal standard and the empirically derived fractionation factors for seawater versus the three DIC species (H_2O–HCO_3^-, H_2O–CO_3^{2-}, H_2O–CO_2). The relative isotopic contribution of each DIC species to DIC $\delta^{18}O$ was determined by the relative abundance of each DIC species, as calculated from TA, DIC, salinity, and temperature of the internal standard (see Beck et al., 2005; Wang et al., 2013). Repeat analyses of the internal standard throughout the sample queue yielded a precision and accuracy better than 0.15 and 0.35‰, respectively.

2.4. Statistical analysis

All statistical analyses and calculations were conducted using the statistical package *R* (*version* 3.0.2). Linear models were used to assess the individual and additive effects of temperature and pCO_2 on the fractionation ($\Delta^{18}O$, $\Delta^{13}C$) between the stable isotopic compositions of the echinoid calcite ($\delta^{18}O_e$, $\delta^{13}C_e$, Table 2) and the stable isotopic compositions of the echinoids' seawater DIC ($\delta^{18}O_{DIC}$, $\delta^{13}C_{DIC}$, Table 2), such that:

$$\Delta^{18}O = \delta^{18}O_e\text{-}\delta^{18}O_{DIC};\ \text{and} \quad (1)$$

$$\Delta^{13}C = \delta^{13}C_e\text{-}\delta^{13}C_{DIC} \quad (2)$$

(notations adapted from Bemis et al., 2000).

This approach accounts for the relatively light $\delta^{13}C_{DIC}$ and $\delta^{13}C_e$ in the high-pCO_2 treatments that result from the relatively light $\delta^{13}C$ composition of the methane-derived CO_2 source-gas (e.g., Suess, 1955). Calcification rates of individual echinoids were also linearly modeled against individual echinoid $\Delta^{18}O$ and $\Delta^{13}C$ to assess the effects of calcification rate on stable isotope fractionation when the effects of

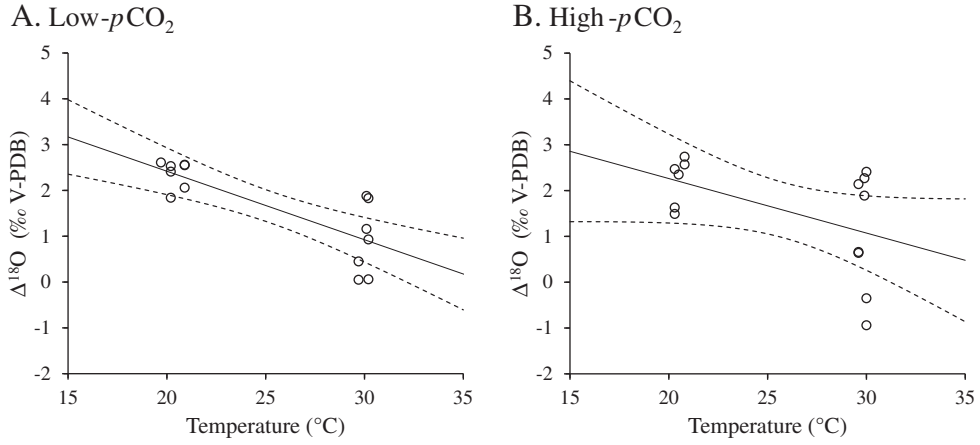

Fig. 1. $\Delta^{18}O$ is negatively correlated with seawater temperature for the echinoid *E. viridis* for low-pCO_2 (A) and high-pCO_2 (B) treatments. Data represent individual echinoid specimens. Solid line is the least-squares linear regression of the data. Dashed lines represent the 95% confidence interval of the regression.

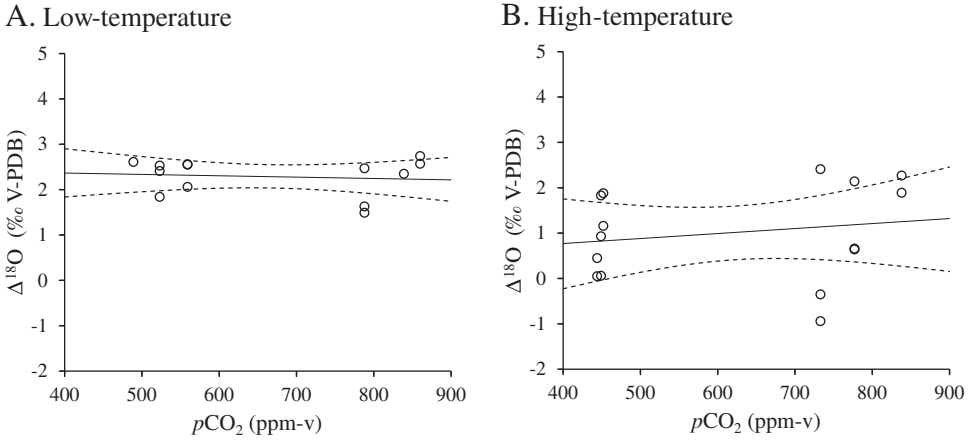

Fig. 2. $\Delta^{18}O$ is not significantly correlated with atmospheric pCO_2 for the echinoid *E. viridis* for low-temperature (A) and high-temperature (B) treatments. Data represent individual echinoid specimens. Solid line is the least-squares linear regression of the data. Dashed lines represent the 95% confidence interval of the regression.

temperature and pCO_2 are controlled for statistically. The statistical significance of these linear models was assessed with ANOVA.

3. Results

3.1. Impacts of temperature and pCO_2 on echinoid $\Delta^{18}O$

The $\Delta^{18}O$ for each echinoid (Table 2) was modeled against seawater temperature (Table 3, Fig. 1) and seawater pCO_2 (Table 3, Fig. 2). Echinoid $\Delta^{18}O$ was inversely correlated with temperature under both low and high-pCO_2 conditions (Fig. 1), but was not correlated with pCO_2 under either the low or high-temperature conditions (Fig. 2). One-way ANOVA confirms that $\Delta^{18}O$ is a statistically significant ($p = 0.0003$) predictor of seawater temperature, whereas two-way ANOVA confirms that neither pCO_2 nor any model involving the additive or interactive effects of temperature and pCO_2 is a statistically significant ($p > 0.05$) predictor of $\Delta^{18}O$ (Table 3, Fig. 2). The linear model describing the relationship between temperature and echinoid $\Delta^{18}O$ is:

$$T \pm SE = (-2.9 \pm 0.7) \times \Delta^{18}O + 30 \pm 1 ^{\circ}C. \quad (3)$$

Substantial interspecimen variability (1–2‰) was observed for echinoid $\Delta^{18}O$ within each of the four experimental treatments (Figs. 1 and 2). Repeated analysis of carbonate reference material yielded a precision better than 0.12‰ for $\delta^{18}O$, indicating that the observed within-treatment variability in $\Delta^{18}O$ reflects true interspecimen variability, rather than analytical error.

3.2. Impacts of temperature and pCO_2 on echinoid $\Delta^{13}C$

The $\Delta^{13}C$ for each echinoid (Table 2) was modeled against pCO_2 (Table 3, Fig. 3) and seawater temperature (Table 3, Fig. 4). Echinoid $\Delta^{13}C$ was positively correlated with pCO_2 under both low- and high-temperature conditions (Fig. 3). Echinoid $\Delta^{13}C$ was not significantly correlated with temperature under the low-pCO_2 conditions, but was significantly negatively correlated with temperature under the high-pCO_2 conditions (Fig. 4). One-way ANOVA (Table 3) confirms that pCO_2 is a statistically significant ($p < 0.0001$) predictor of $\Delta^{13}C$, but that temperature is not ($p > 0.05$). The linear model describing this relationship is:

$$pCO_2 \pm SE = (31 \pm 5) \times \Delta^{13}C + 380 \pm 40 \text{ ppm-v}. \quad (4)$$

However, two-way ANOVA reveals that the additive effects of temperature and pCO_2 are significant ($p < 0.05$) predictors of $\Delta^{13}C$ (Table 3). The linear model describing this relationship is:

$$\Delta^{13}C \pm SE = (-0.2 \pm 0.1) \times T\left(^{\circ}C\right) + (0.019 \pm 0.003) \times pCO_2(\text{ppm-v}) \pm 3\ ‰. \quad (5)$$

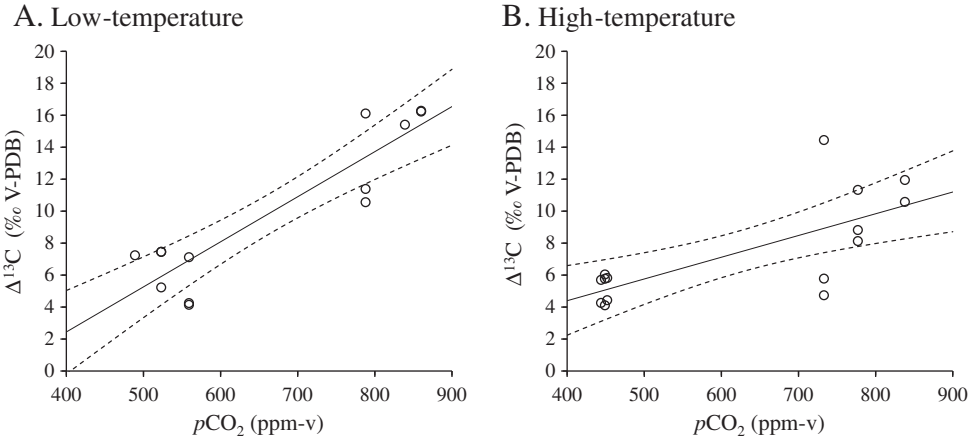

Fig. 3. $\Delta^{13}C$ is positively correlated with atmospheric pCO_2 for the echinoid *E. viridis* for both the low-temperature (A) and high-temperature (B) treatments. Data represent individual echinoid specimens. Solid line is the least-squares linear regression of the data. Dashed lines represent the 95% confidence interval of the regression.

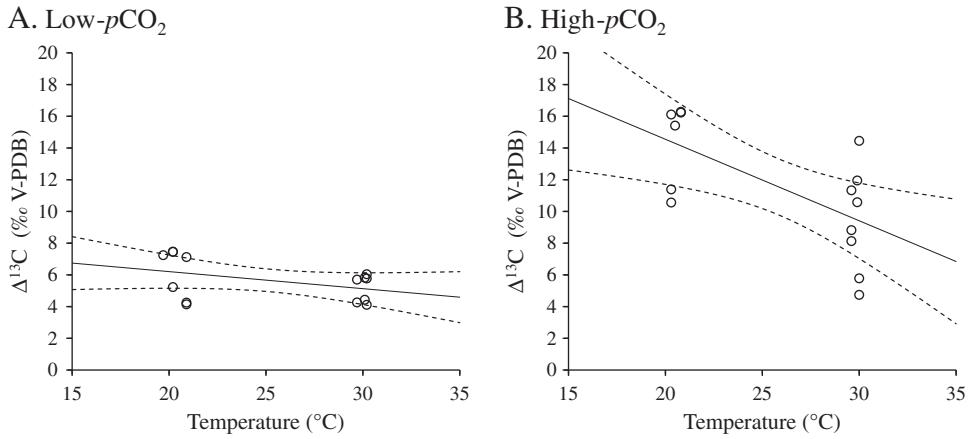

Fig. 4. $\Delta^{13}C$ is not significantly correlated with seawater temperature for the echinoid *E. viridis* under low-pCO_2 (A) but is significantly negatively correlated with seawater temperature under high-pCO_2 (B), suggesting that pCO_2 modulates the seawater temperature–$\Delta^{13}C$ relationship. Data represent individual echinoid specimens. Solid line is the least-squares linear regression of the data. Dashed lines represent the 95% confidence interval of the regression.

Substantial within-treatment variability (4–10‰) was also observed for echinoid $\Delta^{13}C$ within each of the four experimental treatments. Repeated analysis of carbonate reference material yielded a precision better than 0.06‰ for $\delta^{13}C$, indicating that the observed within-treatment variability in $\Delta^{13}C$ reflects true interspecimen variability, rather than analytical error.

3.3. Correlation between echinoid $\Delta^{18}O$ and $\Delta^{13}C$

Echinoid $\Delta^{18}O$ and $\Delta^{13}C$ exhibited clear correlation both across temperature–pCO_2 treatments (Fig. 5) and within temperature–pCO_2 treatments (Fig. 6). Linear modeling (one-way ANOVA; Table 3, Figs. 5 and 6) confirmed a statistically significant ($p = 0.006$) relationship between echinoid $\Delta^{18}O$ and $\Delta^{13}C$, which is described by the following equation:

$$\Delta^{13}C \pm SE = (2.0 \pm 0.7) \times \Delta^{18}O + 5 \pm 1 \text{ ‰}. \quad (6)$$

Sequential multivariate ANOVA (Table 3) reveals that this statistically significant correlation between $\Delta^{18}O$ and $\Delta^{13}C$ persists even when the effects of temperature, pCO_2, and calcification rate (potential drivers of the correlation) are controlled for.

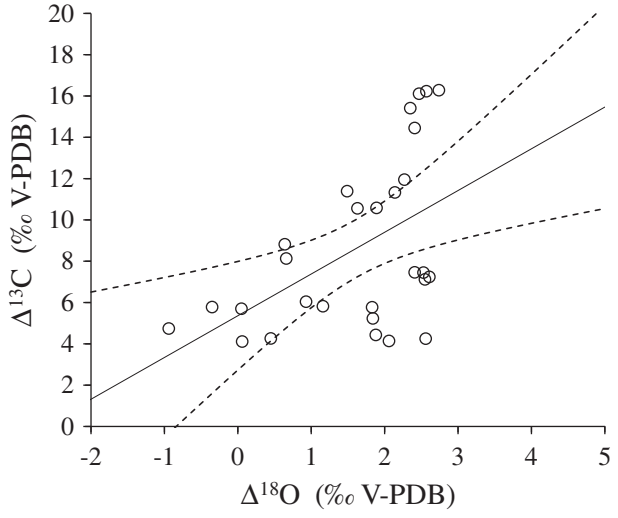

Fig. 5. A significant positive correlation between $\Delta^{18}O$ and $\Delta^{13}C$ for individual *E. viridis* specimens across all treatments may be driven by differences in echinoid metabolism. Solid line is the least-squares linear regression of the data. Dashed lines represent the 95% confidence interval of the regression.

3.4. Impacts of calcification rate on $\Delta^{18}O$ and $\Delta^{13}C$

Courtney et al. (2013) found that calcification rates for the same specimens of *E. viridis* investigated in the present study are positively correlated with temperature (20 to 30 °C) and inversely correlated with atmospheric pCO_2 (448 to 827 ppm-v). These results suggest that the echinoid *E. viridis* will be negatively impacted by CO_2-induced ocean acidification that is predicted for the end of this century and that these effects will be more severe during the colder, winter months and in cooler-water regions (Courtney et al., 2013).

Here, linear models (Table 3) were used to model the effects of calcification rate on $\Delta^{18}O$ (Fig. 7) and $\Delta^{13}C$ (Fig. 8). Three-way ANOVA shows that calcification rate and temperature are statistically significant ($p < 0.05$) predictors of $\Delta^{18}O$, but that pCO_2 is not ($p > 0.05$). The linear model describing this relationship is:

$$\Delta^{18}O(\pm SE) = (-0.02 \pm 0.01) \times \text{calcification rate}(\%) - (0.11 \pm 0.04) \times T(^{\circ}C) + 4 \pm 1 \text{ ‰}. \quad (7)$$

Three-way ANOVA also shows that calcification rate, temperature and pCO_2 are statistically significant ($p < 0.05$) predictors of $\Delta^{13}C$ (Table 3, Fig. 8). The linear model describing this relationship is:

$$\Delta^{13}C(\pm SE) = (-0.08 \pm 0.03) \times \text{calcification rate}(\%) - (0.1 \pm 0.1) \times T\ (^{\circ}C) + (0.016 \pm 0.003) \times pCO_2(\text{ppm-v}) \pm 3 \text{ ‰}. \quad (8)$$

4. Discussion

4.1. Echinoid $\Delta^{18}O$

Results of the present study show that $\Delta^{18}O$ within spines of the tropical echinoid *E. viridis* declines as seawater temperature increases from circa 20 to 30 °C. However, echinoid spine $\Delta^{18}O$ did not exhibit a statistically significant response (Fig. 2, Table 3) to increasing pCO_2 (circa 448 to 827 ppm-v). Adkins et al. (2003) argued that the relationship between seawater temperature and $CaCO_3$ $\delta^{18}O$ is influenced by thermally induced changes in the vibrational frequency of carbonate molecules. Within the discrete biologically mediated calcification sites of corals, which also appear to exist within echinoderms (e.g., Politi et al., 2004; Stumpp et al., 2012; Wilt, 2002), the pH gradient across the site of calcification, the shape and size of the calcification site, and the isotopic composition of respired CO_2 will each introduce 'vital effects' that impact the equilibrium fractionation of stable isotopes within the biogenic $CaCO_3$ (Adkins et al., 2003). The negative correlation in the

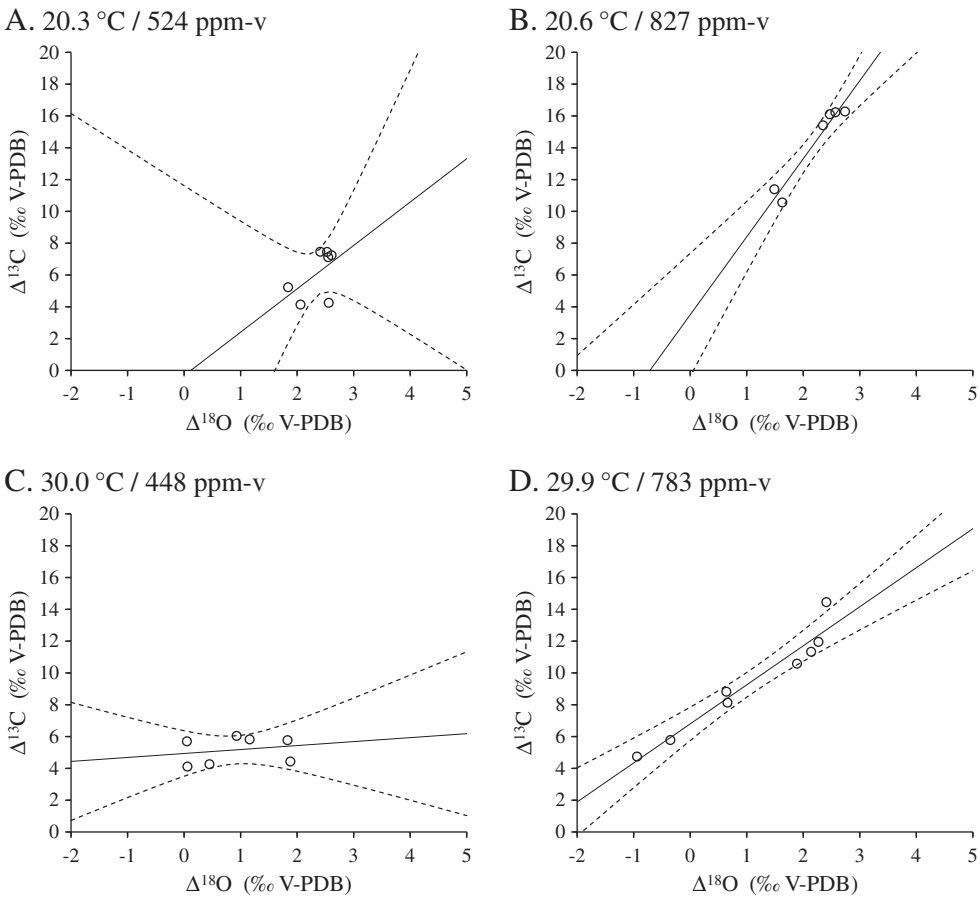

Fig. 6. The strength of the correlation between $\Delta^{18}O$ and $\Delta^{13}C$ for the echinoid *E. viridis* varies among the low-temperature/low-pCO_2 (A), low-temperature/high-pCO_2 (B), high-temperature/low-pCO_2 (C), and high-temperature/high-pCO_2 (D) treatments. This variability may be driven by differences in metabolic rates of the echinoids among the treatments. Data represent individual echinoid specimens. Solid line is the least-squares linear regression of the data. Dashed lines represent the 95% confidence interval of the regression.

present study between echinoid $\Delta^{18}O$ and seawater temperature (Fig. 1, Table 3) is consistent with established relationships between seawater temperature and $CaCO_3$ $\delta^{18}O$, as calculated from equilibrium thermodynamic principles (McCrea, 1950) and as observed within the skeletons of deepwater corals (Adkins et al., 2003) and within the spines and tests of various other species of echinoderms (Baumiller, 2001; Gorzelak et al., 2012; Richter and Bruckschen, 1998; Weber, 1968).

This study also identifies a statistically significant inverse correlation between echinoid $\Delta^{18}O$ and calcification rates (Fig. 7, Table 3), which is consistent with trends observed for scleractinian corals (Erez, 1978; Land et al., 1975; Weil et al., 1981). This inverse relationship between $\Delta^{18}O$ and calcification rate is likely due to kinetic isotope effects associated with CO_2 hydration and hydroxylation, which McConnaughey (1989a) proposed as a mechanism for the simultaneous depletion of ^{13}C and ^{18}O within $CaCO_3$ produced by rapidly growing echinoids and by a range of other rapidly calcifying marine organisms.

4.2. Echinoid $\Delta^{13}C$

Results of the present study show that $\Delta^{13}C$ of spines within the tropical echinoid *E. viridis* is positively correlated with pCO_2. No statistically significant correlation was observed between echinoid spine $\Delta^{13}C$ and the solitary predictor of seawater temperature for all individuals in this experiment, but a significant inverse correlation between $\Delta^{13}C$ and temperature was observed for the high-pCO_2 treatments (Fig. 4, Table 3). Furthermore, multiple regression analysis revealed that the additive effects of pCO_2 and temperature were significantly correlated with $\Delta^{13}C$ (Table 3). The observation that the single-variate effect of temperature on $\Delta^{13}C$ is not significant, while the single-variate effect of pCO_2 on $\Delta^{13}C$ and the multivariate effect of temperature and pCO_2 on $\Delta^{13}C$ are significant, suggests that temperature may influence $\Delta^{13}C$ indirectly via moderation of the more fundamental pCO_2–$\Delta^{13}C$ relationship.

The lack of a statistically significant single-variate relationship between echinoid $\Delta^{13}C$ and seawater temperature in this study was also observed for skeletons of modern crinoids (Weber, 1968). However, the positive correlation between temperature and $\Delta^{13}C$ in the multivariate analysis performed here is consistent with a positive correlation observed between seawater temperature and the skeletal $\delta^{13}C$ of modern ophiuroids (Weber, 1968). These results underscore the complexity of the relationship between temperature and echinoderm $\Delta^{13}C$ (DeNiro and Epstein, 1978; Gorzelak et al., 2012; McConnaughey, 1989a,b; Weber, 1968), which the present study suggests may arise indirectly from the thermal moderation of the more fundamental pCO_2–$\Delta^{13}C$ relationship.

The increase in $\Delta^{13}C$ observed between the low and high-pCO_2 treatments of the present study (up to 16‰) are too high to be explained through equilibrium isotope fractionation and, thus, require one or more mechanisms of kinetic isotope fractionation. One possible mechanism of kinetic isotope fractionation is that the echinoids are utilizing HCO_3^- (e.g., Bijma et al., 1999; Zeebe, 1999; Zhang et al., 1995) in their calcification process, which they may deprotonate by removing protons from their calcifying fluid (e.g., Romanek et al., 1992; Cohen and McConnaughey, 2003; Adkins et al., 2003; Ries, 2011), and which is isotopically heavier than CO_3^{2-} and the total DIC pool. However, this mechanism can only explain a small amount of the total disequilibrium (up to 16‰) observed in the present study, as $\delta^{13}C$ of HCO_3^- is only enriched by 1–2‰ relative to $\delta^{13}C$ of CO_3^{2-} and the total DIC pool of seawater.

Calcification rate is another potential driver of kinetic isotope effects. Indeed, a statistically significant inverse correlation between echinoid

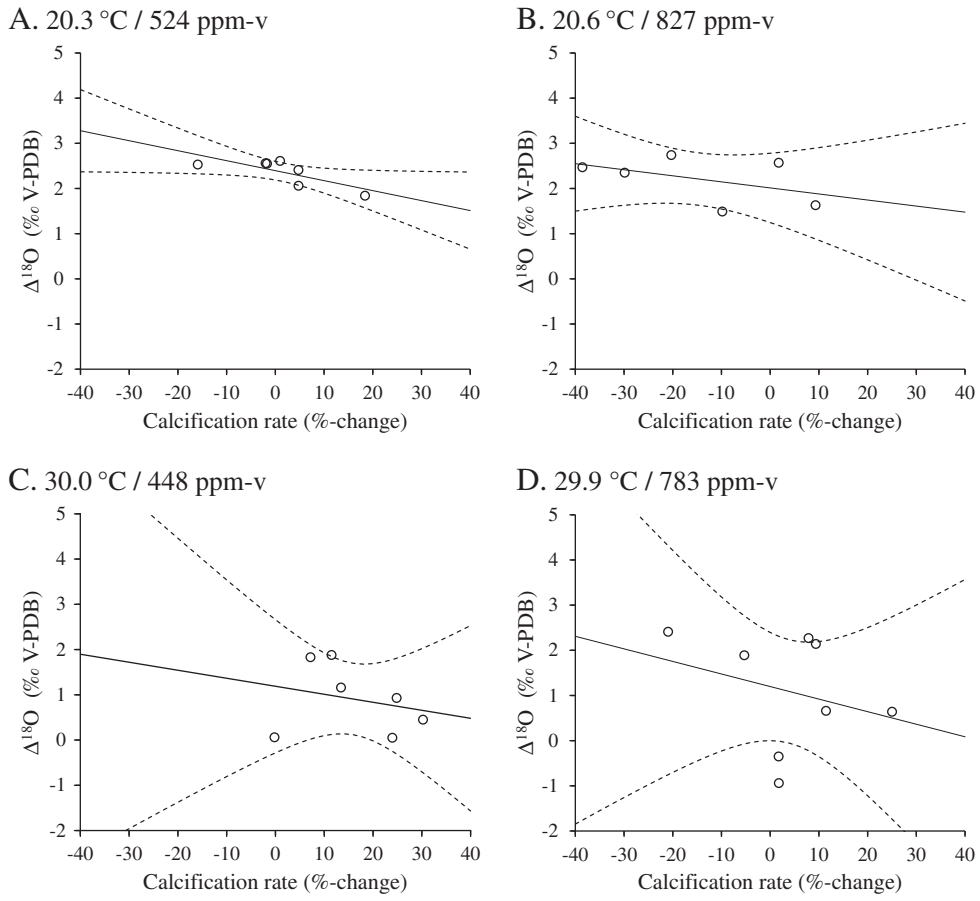

Fig. 7. The strength of the correlation between $\Delta^{18}O$ and calcification rate for the echinoid *E. viridis* varies among the low-temperature/low-pCO_2 (A), low-temperature/high-pCO_2 (B), high-temperature/low-pCO_2 (C), and high-temperature/high-pCO_2 (D) treatments. Data represent individual echinoid specimens. Solid line is the least-squares linear regression of the data. Dashed lines represent the 95% confidence interval of the regression.

calcification rate and $\Delta^{13}C$ was observed across treatments (with the effects of temperature and pCO_2 on $\Delta^{13}C$ controlled for through ANOVA; Fig. 8, Table 3). The direction and magnitude of this correlation is consistent with the kinetic isotope effects of calcification rate observed in various calcifying taxa by McConnaughey (1989a, b), in crinoids (Gorzelak et al., 2012), in deepwater scleractinian corals (Adkins et al., 2003), and in planktonic foraminifera (Bijma et al., 1999).

A third potential driver of kinetic isotope fractionation, related to the calcification mechanism discussed above, is selective dissolution of $CaCO_3$ molecules containing isotopically lighter ^{12}C-isotopes ($Ca–^{12}CO_3$ bonds are weaker than $Ca–^{13}CO_3$ bonds, as bond strength is proportional to ionic mass; Bigeleisen and Mayer, 1947), which would effectively enrich the remaining undissolved $CaCO_3$ in ^{13}C. Skidmore et al. (2004) showed that partial dissolution can enrich the $\delta^{13}C$ composition of carbonate sediments by 5–15‰, which is consistent with the relatively large isotope fractionation (up to 16‰) observed for the high-CO_2 treatments, where calcite dissolution rates were highest and the resulting kinetic isotope effects would have been greatest. Dissolution-driven isotope fractionation could potentially even operate within specimens exhibiting net calcification, as recent work suggests that net calcification within marine calcifiers is commonly the product of co-occurring gross calcification and gross dissolution of their shell or skeleton—the balance of which determines whether they are calcifying or dissolving on a net basis (e.g., Ries, 2011; Rodolfo-Metalpa et al., 2011). However, further research is needed to assess the impact of dissolution on stable isotope fractionation within biogenic carbonates.

It should be noted here that echinoids reared under the same experimental pCO_2–temperature conditions in this study exhibited substantial variability in $\Delta^{13}C$ (Figs. 3 and 4) compared with the observed variability in $\Delta^{18}O$ (Figs. 1 and 2). Although prior work suggests that echinoderm diet impacts skeletal $\Delta^{13}C$ by as much as 3‰ (DeNiro and Epstein, 1978), diet should not have introduced much interspecimen variability in $\Delta^{13}C$ as the echinoids were fed equal amounts of food that had a narrow range of $\delta^{13}C$ composition (range: −24.91 to −26.08‰; avg. = −25.7‰, SE = 0.1‰). The significant correlation between calcification rate and $\Delta^{13}C$ suggests that the interspecimen variability in $\Delta^{13}C$ within temperature–pCO_2 treatments results from the kinetic isotope effects of within-treatment variability in calcification and/or dissolution rates.

4.3. Echinoid $\Delta^{18}O$ vs. $\Delta^{13}C$

Echinoid $\Delta^{18}O$ and $\Delta^{13}C$ were significantly positively correlated (Figs. 5 and 6; Table 3). A potential driver of this correlation is echinoid calcification rate, as $\Delta^{18}O$ and $\Delta^{13}C$ responded in the same direction to calcification rates among treatments (Figs. 7 and 8, Table 3). However, the correlation between $\Delta^{18}O$ and $\Delta^{13}C$ persists even when the effects of temperature, pCO_2, and calcification rate are controlled for through sequential multivariate ANOVA (Table 3), suggesting that the correlation is driven by some factor(s) not quantified in the present experiment. Weber (1968) observed a similar correlation between $\delta^{13}C$ and $\delta^{18}O$ within ophiuroids that he attributed to mineralization of respired CO_2, which was enriched in both ^{12}C and ^{16}O relative to the ambient seawater. Thus, the positive correlation between $\Delta^{18}O$ and $\Delta^{13}C$ observed in the present study may result from interspecimen variations in metabolic rates (not quantified in the present study), such that echinoid specimens with faster metabolisms would consume more food, which is isotopically lighter than seawater (see Section 4.2), and

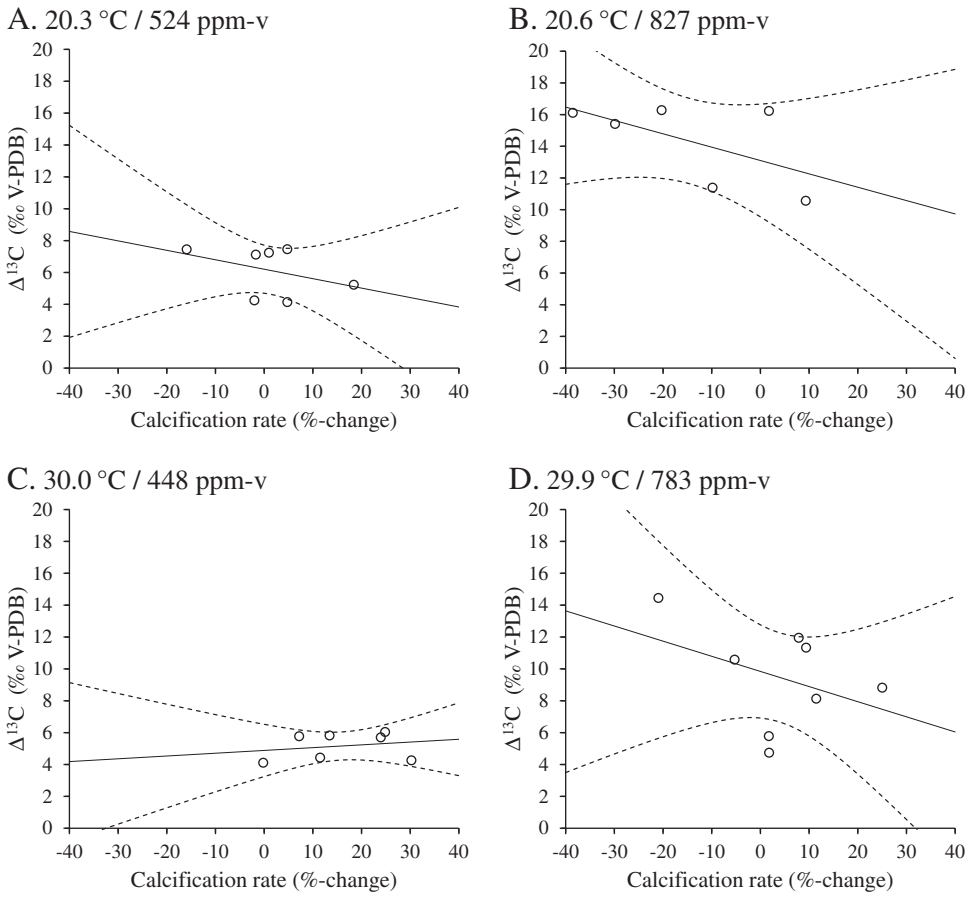

Fig. 8. The strength of the correlation between $\Delta^{13}C$ and calcification rate for the echinoid *E. viridis* varies among the low-temperature/low-pCO_2 (A), low-temperature/high-pCO_2 (B), high-temperature/low-pCO_2 (C), and high-temperature/high-pCO_2 (D) treatments. Data represent individual echinoid specimens. Solid line is the least-squares linear regression of the data. Dashed lines represent the 95% confidence interval of the regression.

incorporate more isotopically light respired-CO_2 into their mineralized structures.

4.4. Echinoid $\Delta^{18}O$ and $\Delta^{13}C$ as proxies of paleo-temperature and paleo-pCO_2

The present study identified a strong negative correlation between seawater temperature and $\Delta^{18}O$ within spines of the echinoid *E. viridis* (Fig. 1, Table 3). This observation is consistent with negative correlations identified between $\Delta^{18}O$ and seawater temperature for modern ophiuroids (Weber, 1968), modern crinoids (Baumiller, 2001), and extant crinoids (Gorzelak et al., 2012).

This relationship between echinoid $\delta^{18}O$ and seawater temperature may be useful in reconstructing past seawater temperatures from the $\delta^{18}O$ composition of analogous skeletal elements of fossil echinoderms as long as $\delta^{18}O_{DIC}$ is known (see the Phanerozoic $\delta^{18}O$ time-curve; Veizer et al., 1999). This paleo-temperature proxy for *E. viridis* can be defined by the following algorithm:

$$T \pm SE = (-2.9 \pm 0.7) \times \left(\delta^{18}O_e - \delta^{18}O_{DIC}\right) + 30 \pm 1 °C. \quad (9)$$

The apparent lack of relationship between atmospheric pCO_2 (seawater pH) and echinoid $\Delta^{18}O$ observed in the present study (Fig. 2, Table 3) is also supportive of the application of the echinoderm-based $\delta^{18}O$ proxy of paleoseawater temperature, as it suggests that paleo-atmospheric pCO_2 and paleoseawater pH need not be known (or corrected for) over the interval that the paleothermometer is applied. However, the observed impact of calcification rate on echinoid $\Delta^{18}O$ and $\Delta^{13}C$ suggests that paleoceanographic reconstructions derived from these proxies in fossil echinoids could be improved by incorporating the effects of calcification rate.

The present study also found that temperature and atmospheric pCO_2 had a statistically significant effect on echinoid $\Delta^{13}C$, with pCO_2 being the primary driver (i.e., pCO_2 was statistically significant as a single-variate predictor of $\Delta^{13}C$) and temperature being a secondary driver (i.e., temperature was only statistically significant as a multivariate predictor of $\Delta^{13}C$ in conjunction with pCO_2; Table 3). Although the observed secondary relationship between temperature and echinoid $\Delta^{13}C$ is not strong enough to support its use in paleotemperature reconstruction, the observed primary relationship between pCO_2 and echinoid $\Delta^{13}C$ may be sufficiently robust to support reconstruction of paleo-pCO_2, as long as seawater temperature and $\delta^{13}C_{DIC}$ are known. This paleo-pCO_2 proxy for *E. viridis* can be defined by the following algorithm:

$$pCO_2(\text{ppm-v}) = \frac{\left(\delta^{13}C_e - \delta^{13}C_{DIC}\right) + (0.2 \pm 0.1) \times T(°C) \pm 3}{0.019 \pm 0.003}. \quad (10)$$

Substitution of the $\delta^{18}O$-based temperature proxy (Eq. (3)) for *E. viridis* for the temperature factor in the paleo-pCO_2 proxy yields:

$$pCO_2(\text{ppm-v}) = \frac{\left(\delta^{13}C_e - \delta^{13}C_{DIC}\right) + (0.2 \pm 0.1) \times \left[(-2.9 \pm 0.7) \times \left(\delta^{18}O_e - \delta^{18}O_{DIC}\right) + 30 \pm 1\right] \pm 3}{0.019 \pm 0.003}. \quad (11)$$

As for any fossil-based $\delta^{18}O$- or $\delta^{13}C$-paleoceanographic reconstruction, the fossils hosting the isotope paleo-proxies must be sufficiently

well-preserved so as to retain close to their primary isotopic signatures. Work focused on reconstructing ancient seawater Mg/Ca from the Mg/Ca of fossil echinoderms (Dickson, 2002, 2004) and a recent study documenting high-quality preservation of echinoderm-specific organic molecules within fossil crinoids of lower Mississippian age (340 Ma; O'Malley et al., 2013) suggest that echinoderms may be particularly well suited for preserving biogeochemical proxies. Dickson (2002, 2004) attributed this to the encapsulation of their fossilized skeletal elements by relatively hydrophobic organic matter that seals them off from diagenetic waters that would otherwise reset their primary geochemical signatures.

Echinoderms are well-suited for paleotemperature reconstructions due to their long fossil record dating back to the Lower Cambrian (Paul and Smith, 1984), their relatively high abundance and ubiquitous distribution across most marine facies (Lebrato et al., 2010), their generally high quality of preservation in the fossil record (Dickson, 2002, 2004; O'Malley et al., 2013), their empirically demonstrated ability to record seawater temperatures in the $\delta^{18}O$ of their spines (Weber, 1968; Baumiller, 2001; Gorzelak et al., 2012; this study), and their apparent lack of correlation between skeletal $\delta^{18}O$ and pCO_2 (pH). The observed relationship between $\Delta^{13}C$ and pCO_2, although complicated by the apparently moderating effects of temperature, should compel future investigations into potential echinoid-based $\delta^{13}C$-proxies of paleo-atmospheric pCO_2.

The application of these echinoid-based paleoceanographic proxies must be considered within the context of other independent proxies of paleotemperature and paleo-pCO_2 to control for the potential influences of diagenetic alteration, paleoseawater salinity, diet, calcification rate, and local river water input on echinoid calcite $\delta^{18}O$ and $\delta^{13}C$ (Richter and Bruckschen, 1998). Although calcification rate was shown to significantly impact both $\delta^{18}O$ and $\delta^{13}C$ of the echinoid tests (Eqs. (7), (8); Table 3), the magnitude of these effects were generally small compared to the primary factors of temperature and/or pCO_2 (Table 3). This, combined with the difficulty in estimating calcification rates of fossils, prompted exclusion of the calcification rate variable from the paleo-proxy regressions presented above (Eqs. (9), (10), (11)). If, however, calcification rates can be reasonably estimated for fossil echinoids employed in the paleo-reconstructions, e.g., through analysis of seasonal or annual banding within the skeleton, then paleoceanographic reconstructions derived from fossil echinoid $\Delta^{18}O$ and $\Delta^{13}C$ could be improved by incorporating the effects of echinoid growth rate (Eqs. (7) and (8); Table 3).

Phylogenetic differences in the temperature–$\Delta^{18}O$ and pCO_2–$\Delta^{13}C$ relationships of echinoderms through time may also complicate the application of these paleoceanographic proxies to evolutionarily distal echinoderms (Weber and Raup, 1968). Nevertheless, application of the *E. viridis* $\Delta^{18}O$-paleothermometer and $\Delta^{13}C$-paleo-pCO_2-proxy to analogous well-preserved skeletal elements of closely related echinoderms, considered within the framework of the seawater $\delta^{18}O_{DIC}$ and $\delta^{13}C_{DIC}$ time-curves, may yield novel records of seawater temperature and atmospheric pCO_2 throughout much of Phanerozoic time.

5. Conclusions

Analysis of stable isotopes of oxygen ($\delta^{18}O$) and carbon ($\delta^{13}C$) within spines of the tropical echinoid *E. viridis* reared in replicated laboratory experiments under different temperature and pCO_2 conditions reveal that: (1) $\Delta^{18}O$ has a significant inverse relationship with temperature and no significant relationship with pCO_2; (2) $\Delta^{13}C$ has a significant positive relationship with pCO_2 (major) and a significant inverse relationship with temperature (minor); (3) echinoid calcification rate has significant inverse relationships with both $\Delta^{18}O$ and $\Delta^{13}C$; and (4) $\Delta^{18}O$ is significantly positively correlated with $\Delta^{13}C$, even after controlling for the effects of pCO_2, temperature, and calcification rate. These results are consistent with prior studies suggesting that fossil echinoderm $\Delta^{18}O$ holds promise as a geochemical proxy of paleo-temperature that could be applied throughout much of Phanerozoic time and also suggest that echinoid $\Delta^{13}C$ merits further investigation as a potential proxy of paleo-atmospheric pCO_2. However, the observation that calcification rate significantly impacts echinoid $\Delta^{18}O$ and $\Delta^{13}C$ suggests that paleoceanographic reconstructions derived from fossil echinoid $\Delta^{18}O$ and $\Delta^{13}C$ could be improved by incorporating the effects of echinoid growth rate.

Acknowledgments

We acknowledge A. Brandt for assisting with urchin culturing and I. Westfield for assisting with seawater analysis. This work was supported with funding from the National Science Foundation (OCE-1357665, OCE-1429373, OCE-1437371 and OCE-1459706 to JBR) and the National Oceanographic and Atmospheric Administration (NA13OAR4310186 and NA14NMF4540072 to JBR). This is contribution number 324 of the Marine Science Center at Northeastern University.

References

Adkins, J.F., Boyle, E.A., Curry, W.B., Lutringer, A., 2003. Stable isotopes in deep-sea corals and a new mechanism for "vital effects". Geochim. Cosmochim. Acta 67, 1129–1143.
Atkinson, M.J., Bingham, C., 1998. Elemental composition of commercial seasalts. J. Aquaric. Aquat. Sci. 8, 39–43.
Baumiller, T.K., 2001. Light stable isotope geochemistry of the crinoid skeleton and its use in biology and paleobiology. In: Barker, M. (Ed.), Echinoderms 2000. Balkema, Lisse, pp. 107–112.
Beck, W.C., Grossman, E.L., Morse, J.W., 2005. Experimental studies of carbon isotopic fractionation in the carbonic acid system at 15°, 25°, and 40 °C. Geochim. Cosmochim. Acta 14, 3493–3503.
Bemis, B.E., Spero, H.J., Lea, D.W., Bijma, J., 2000. Temperature influence on the carbon isotopic composition of *Globigerina bulloides* and *Orbulina universa* (planktonic foraminifera). Mar. Micropaleontol. 38, 213–228.
Berner, R.A., 1990. Atmospheric carbon dioxide levels over Phanerozoic time. Science 249, 1382–1386.
Bigeleisen, J., Mayer, M.G., 1947. Calculation of equilibrium constants for isotopic exchange reactions. J. Chem. Phys. 15, 261–267.
Bijma, J., Spero, H.J., Lea, D.W., 1999. Reassessing foraminiferal stable isotope geochemistry: impact of the oceanic carbonate system (experimental results). Use of Proxies in Paleoceanography: Examples from the South Atlantic, pp. 489–512.
Cohen, A.L., McConnaughey, T.A., 2003. Geochemical perspectives on coral mineralization. Rev. Mineral. Geochem. 54, 151–187.
Courtney, T., Westfield, I., Ries, J.B., 2013. CO_2-induced ocean acidification impairs calcification in the tropical urchin *Echinometra viridis*. J. Exp. Mar. Biol. Ecol. 440, 169–175.
DeNiro, M., Epstein, S., 1978. Influence of diet on the distribution of carbon isotopes in animals. Geochim. Cosmochim. Acta 42, 495–506.
Dickson, J.A.D., 2002. Fossil echinoderms as monitor of the Mg/Ca ratio of Phanerozoic oceans. Science 298, 1222–1224.
Dickson, J.A.D., 2004. Echinoderm skeletal preservation: Calcite-aragonite seas and the Mg/Ca ratio of Phanerozoic oceans. J. Sediment. Res. 74, 355–365.
Emiliani, C., 1955. Pleistocene temperatures. J. Geol. 63, 538–578.
Erez, J., 1978. Vital effect on stable-isotope composition seen in foraminifera and coral skeletons. Nature 273, 199–202.
Gorzelak, P., Stolarski, J., Malkowski, K., Meibom, A., 2012. Stable carbon and oxygen isotope compositions of extant crinoidal echinoderm skeletons. Chem. Geol. 291, 132–140.
Hasiuk, F.J., Lohmann, K.C., 2008. Mississippian paleocean chemistry from biotic and abiotic carbonate, Muleshoe Mound, Lake Valley Formation, New Mexico, USA. J. Sediment. Res. 78, 147–160.
Land, L.S., Lang, J.C., Barnes, D.J., 1975. Extension Rate: A primary control on the isotopic composition of West Indian (Jamaican) scleractinian reef coral skeletons. Mar. Biol. 33, 221–233.
Lebrato, M., Iglesias-Rodriguez, D., Feely, R., Greeley, D., Jones, D., et al., 2010. Global contribution of echinoderms to the marine carbon cycle: a reassessment of the oceanic $CaCO_3$ budget and the benthic compartments. Ecol. Monogr. 80, 441–467.
Lewis, E., Wallace, D.W.R., 1998. CO2SYS: Program developed for CO_2 system calculations, ORNL/CDIAC-105. Carbon Dioxide Information Analysis Center, Oak Ridge National Laboratory, U.S. Department of Energy, Oak Ridge, Tennessee.
McConnaughey, T., 1989a. ^{13}C and ^{18}O isotopic disequilibrium in biological carbonates: II in vitro simulation of kinetic isotope effects. Geochim. Cosmochim. Acta 53, 163–171.
McConnaughey, T., 1989b. 13C and 18O isotopic disequilibrium in biological carbonates: I. Patterns. Geochim. Cosmochim. Acta 53, 151–162.
McCrea, J.M., 1950. On the isotope chemistry of carbonates and a paleotemperature scale. J. Chem. Phys. 18, 849–857.
McPherson, B., 1969. Studies on the biology of the tropical urchins, *Echinometra lucunter* and *Echinometra viridis*. Bull. Mar. Sci. 19, 194–213.
Mucci, A., 1983. The solubility of calcite and aragonite in seawater at various salinities, temperatures, and one atmosphere total pressure. Am. J. Sci. 283, 780–799.
O'Malley, C.E., Ausich, W.I., Chin, Y., 2013. Isolation and characterization of the earliest taxon-specific organic molecules (Mississippian, Crinoidea). Geology 41, 347–350.

Paul, C.R.C., Smith, A.B., 1984. The early radiation and phylogeny of echinoderms. Biol. Rev. 59, 443–481.
Petit, J.R., Jouzel, J., Raynaud, D., Barkov, N.I., Barnola, J.M., Basile, I., Bender, M., Chappellaz, J., Davis, M., Delaygue, G., Demotte, M., Kotlyakov, V.M., Legrand, M., Lipenkov, V.Y., Lorius, C., Pépin, L., Ritz, C., Saltzman, E., Stievenard, M., 1999. Climate and atmospheric history of the past 420,000 years from the Vostok ice core, Antarctica. Nature 399, 429–436.
Politi, Y., Arad, T., Klein, E., Weiner, S., Addadi, L., 2004. Sea urchin spine calcite forms via a transient amorphous calcium phase. Science 306, 1161–1164.
Richter, D.K., Bruckschen, P., 1998. Geochemistry of recent tests of *Echinocyamus pusillus*: constraints for temperature and salinity. Carbonates Evaporites 13, 157–167.
Ries, J.B., 2011. A physicochemical framework for interpreting the biological calcification response to CO_2-induced ocean acidification. Geochim. Cosmochim. Acta 75, 4053–4064.
Ries, J.B., Cohen, A.L., McCorkle, D.C., 2009. Marine calcifiers exhibit mixed responses to CO_2-induced ocean acidification. Geology 37, 1131–1134.
Rodolfo-Metalpa, R., Houlbrèque, F., Tambutté, É., Boisson, F., Baggini, C., Patti, F.P., Jeffree, R., Fine, M., Foggo, A., Gattuso, J.-P., Hall-Spencer, J.M., 2011. Coral and mollusk resistance to ocean acidification adversely affected by warming. Nat. Clim. Chang. 1, 308–312.
Romanek, C.S., Grossman, E.L., Morse, J.W., 1992. Carbon isotopic fractionation in synthetic aragonite and calcite: effects of temperature and precipitation rate. Geochim. Cosmochim. Acta 56, 419–430.
Roy, R.N., Roy, L.N., Vogel, K.M., Porter-Moore, C., Pearson, T., Good, C.E., Millero, F.J., Campbell, D.M., 1993. The dissociation constants of carbonic acid in seawater at salinities 5 to 45 and temperatures 0 to 45 °C. Mar. Chem. 44, 249–267.
Shackleton, N.J., Hall, M.A., Line, J., Shuxi, C., 1983. Carbon isotope data in core V19-30 confirm reduced carbon dioxide concentration in the ice age atmosphere. Nature 306, 319–322.
Skidmore, M., Sharp, M., Tranter, M., 2004. Kinetic isotopic fractionation during carbonate dissolution in laboratory experiments: implications for detection of microbial CO_2 signatures using δ^{13}C-DIC. Geochim. Cosmochim. Acta 68, 4309–4317.
Stumpp, M., Hua, M.Y., Melzner, F., Gutowska, M.A., Dorey, N., Himmerkus, N., Holtmann, W.C., Dupont, S.T., Thorndyke, M.C., Bleich, M., 2012. Acidified seawater impacts sea urchin larvae pH regulatory systems relevant for calcification. PNAS 109, 18192–18197.
Suess, H.E., 1955. Radiocarbon concentration in modern wood. Science 122, 415–416.
Veizer, J., Ala, D., Azmy, K., Bruckschen, P., Buhl, D., Bruhn, F., Carden, G.A.F., Diener, A., Ebneth, S., Godderis, Y., Jasper, T., Korte, C., Pawellek, F., Podlaha, O.G., Strauss, H., 1999. $^{87}Sr/^{86}Sr$, $\delta^{13}C$, and $\delta^{18}O$ evolution of Phanerozoic seawater. Chem. Geol. 161, 59–88.
Veizer, J., Godderis, Y., Francois, L.M., 2000. Evidence for decoupling of atmospheric CO_2 and global climate during the Phanerozoic era. Nature 408, 698–701.
Wang, Z., Gaetani, G., Liu, C., Cohen, A., 2013. Oxygen isotope fractionation between aragonite and seawater: developing a novel kinetic oxygen isotope fractionation model. Geochim. Cosmochim. Acta 117, 232–251.
Weaver, P.P.E., Neil, H., Carter, L., 1997. Sea surface temperature estimates from the Southwest Pacific based on planktonic foraminifera and oxygen isotopes. Palaeogeogr. Palaeoclimatol. Palaeoecol. 131, 241–256.
Weber, J.N., 1968. Fractionation of the stable isotopes of carbon and oxygen in marine calcareous organisms—the *Asteroidea*, *Ophiuroidea* and *Crinoidea*. Geochim. Cosmochim. Acta 32, 33–70.
Weber, J.N., 1973. Temperature dependence of magnesium in echinoderm and asteroid skeletal calcite: a reinterpretation of its significance. J. Geol. 81, 543–556.
Weber, J.N., Raup, D.M., 1966. Fractionation of the stable isotopes of carbon and oxygen in marine calcareous organisms—the *Echinoidea*. Part 1. Variation of C^{13} and O^{18} content within individuals. Geochim. Cosmochim. Acta 30, 681–703.
Weber, J.N., Raup, D.M., 1968. Composition of C^{13}/C^{12} and O^{18}/O^{16} in the skeletal calcite of recent and fossil echinoids. J. Paleontol. 42, 37–50.
Weil, S.M., Buddemeier, R.W., Smith, S.V., Kroopnick, P.M., 1981. The stable isotopic composition of coral skeletons: Control by environmental variables. Geochim. Cosmochim. Acta 45, 1147–1153.
Wilt, F.H., 2002. Biomineralization of the spicules of sea urchin embryos. Zool. Sci. 19, 253–261.
Zeebe, R.E., 1999. An explanation of the effect of seawater carbonate concentration on foraminiferal oxygen isotopes. Geochim. Cosmochim. Acta 63, 2001–2007.
Zeebe, R.E., Wolf-Gladrow, 2001. CO_2 in Seawater: Equilibrium, Kinetics, Isotopes. Elsevier Oceanography Series 65, p. 346 (Amsterdam).
Zhang, J., Quay, P.D., Wilbur, D.O., 1995. Carbon isotope fractionation during gas–water exchange and dissolution of CO_2. Geochim. Cosmochim. Acta 59, 107–114.